# SUPPLEMENTARY DATA

## Supplementary figure legends

### Figure. S1. Hh signaling is not perturbed in *lgl* tumors

(A) Gene Set Enrichment Analysis (GSEA) (Subramanian et al., 2005), plot displaying absence of Hh-pathway enrichment in *lgl* mosaic tumors. GSEA provides a quantitative measure for the enrichment status of a set of predefined genes between two phenotypes. A gene set is considered statistically enriched at a $p<0.05$; an FDR (false discovery rate) and a more conservative FWER of <0.05 (see, Khan et al., 2013). GSEA analysis of the transcriptome of *lgl* mosaics wing disc (http://www.ebi.ac.uk/arrayexpress/experiments/E-MEXP-2753/, (Khan et al., 2013) generated in a *Minute* genetic background does not reveal significant enrichment of the Hh signaling pathway. (B-C) Mosaic wing imaginal disc displaying *lgl* mutant clones (non-green) generated in a *Minute* genetic background and marked by the absence of Lgl do not display gain of Ptc distally where these do not transform (C, blue stars) or in the hinge domain where these transform (arrowhead). Neoplastic transformation was assayed by the disrupted F actin in the lgl clones (arrow in B). (D) *lgl* mutant clones (marked by absence β-galactosidase) do not show any change in the levels of Dpp target, pMAD (blue stars, D). Abbreviation: A= Anterior, P=Posterior, in all figures. Scale bars 100 μm.

### Figure S2. Ectopic gain of En in the anterior wing forms *de novo* A/P boundaries and activates Hh signaling.

(A) Hh ligand-secreting, *UAS-en* clones in the anterior [A] wing compartment exhibit cell autonomous loss of Ci and non-cell autonomous gain of Ci around the clones (arrowheads, see (Dominguez et al., 1996)). (B) *UAS-en* clones in the anterior compartment with gain of Hh target Ptc outside the clone boundary (arrowhead, also see, Zecca et al., 1995). (C) The Dpp target pMAD (C, arrowhead, see Tanimoto et al., 2000) is activated both within and outside the clone boundary (dotted outline). Boxed areas in the middle panels are shown at a higher magnification on the right. Scale bars 100 μm.

### Figure S3. Hh-sending *lgl* mutant clones undergo neoplastic transformation in the anterior compartment.

(A) Anterior [A] and posterior [P] compartments of the leg and haltere imaginal discs displaying expression of En and Ci. (B) Hh target, Ptc (G), is seen in the anterior cells abutting the A/P boundary.

(C-D) Hh ligand-sending *lgl* clones (*lgl UAS-en*) undergo neoplastic transformations (arrow) selectively in the anterior compartments of haltere (G) and leg (H) imaginal discs, and induce the Hh target, Ptc (arrow), in cell abutting the clone boundary. Scale bars 100 μm.

**Figure S4. Hh-sending *lgl* mutant clones display hyperplasia in surrounding tissue**

*lgl UAS-en* clone (GFP) anterior to the MF (boxed area) display hyperplasia in surrounding tissue (arrowhead), as seen by characteristic folds of the surrounding epithelium (grey, F-actin). Boxed region has been magnified in the far right. Scale bars 100 μm.

**Figure S5. Hh-receiving *lgl* mutant clones transform in the posterior compartment.**

(A-C) Hh ligand-receiving clones, *UAS-ci,* activate Hh targets in only the posterior (P) wing compartment. (A) *UAS-ci* clones do not exhibit loss of En (arrow). (B) *UAS-ci* clones in the posterior wing compartment display cell autonomous gain of Hh target, Ptc (arrow), and (C) a Dpp target, pMAD (arrow). (D-E) Hh ligand-receiving *lgl* clones (*lgl UAS-ci*) undergo neoplastic transformation (arrow) selectively in the posterior compartments of haltere (D) and leg (E) imaginal discs, and display cell autonomous gain of Hh target, Ptc (D, E). Scale bars 100 μm.

FIGURE S1

A

Hh pathway Enrichment plot

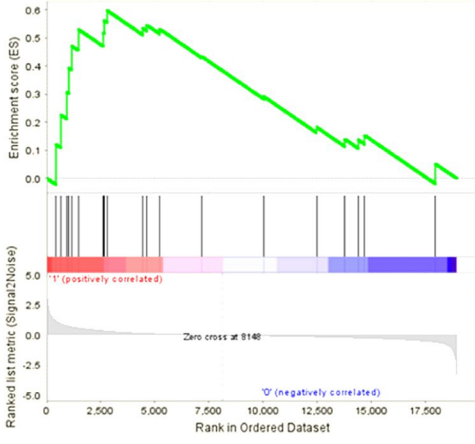


Enrichment profile
Hits
Ranking metric score

Normalized Enrichment Score: 1.526
Nominal p-value: 0.052
FDR-q Value: 0.060
FWER p value 0.999

*lgl* mosaic

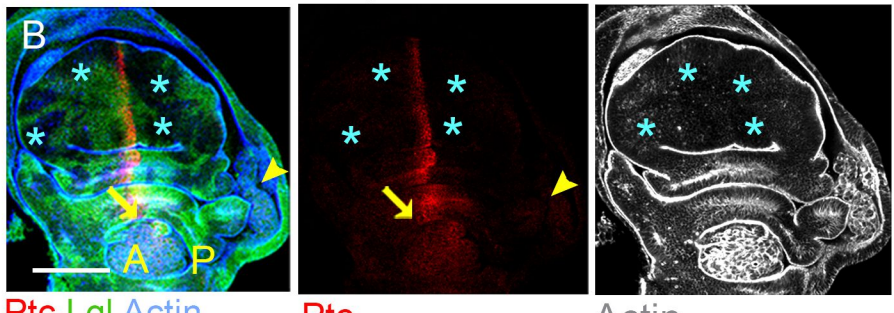


Ptc Lgl Actin



Ptc



Actin

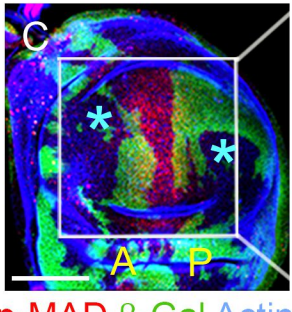


p-MAD β-Gal Actin

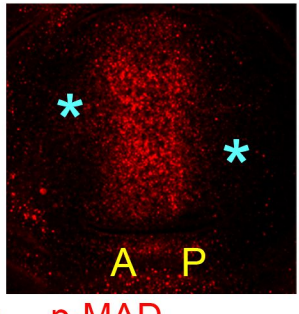


p-MAD

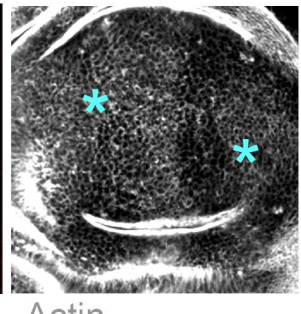

Actin

FIGURE S2

Hh-sending *UAS-en* clones

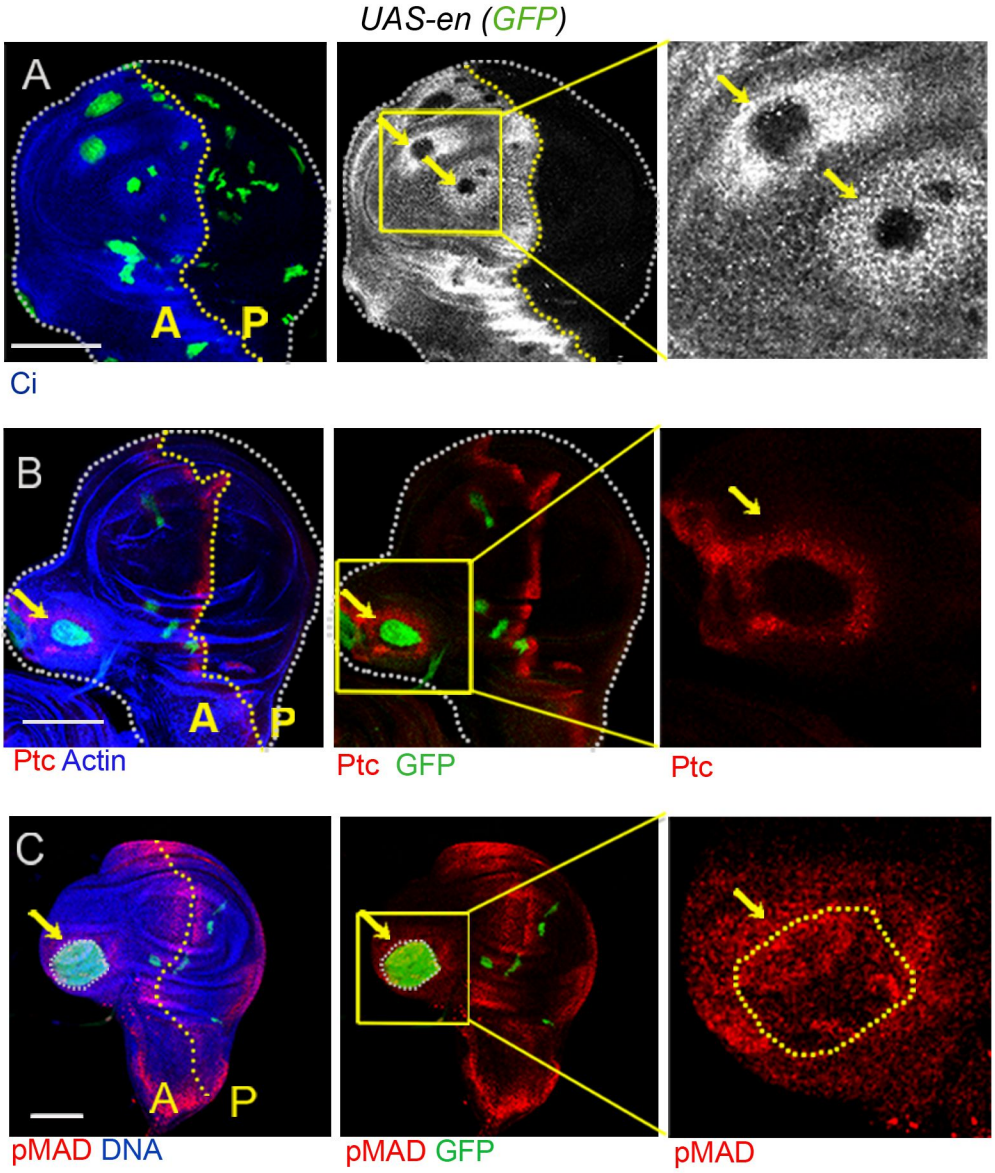

FIGURE S3

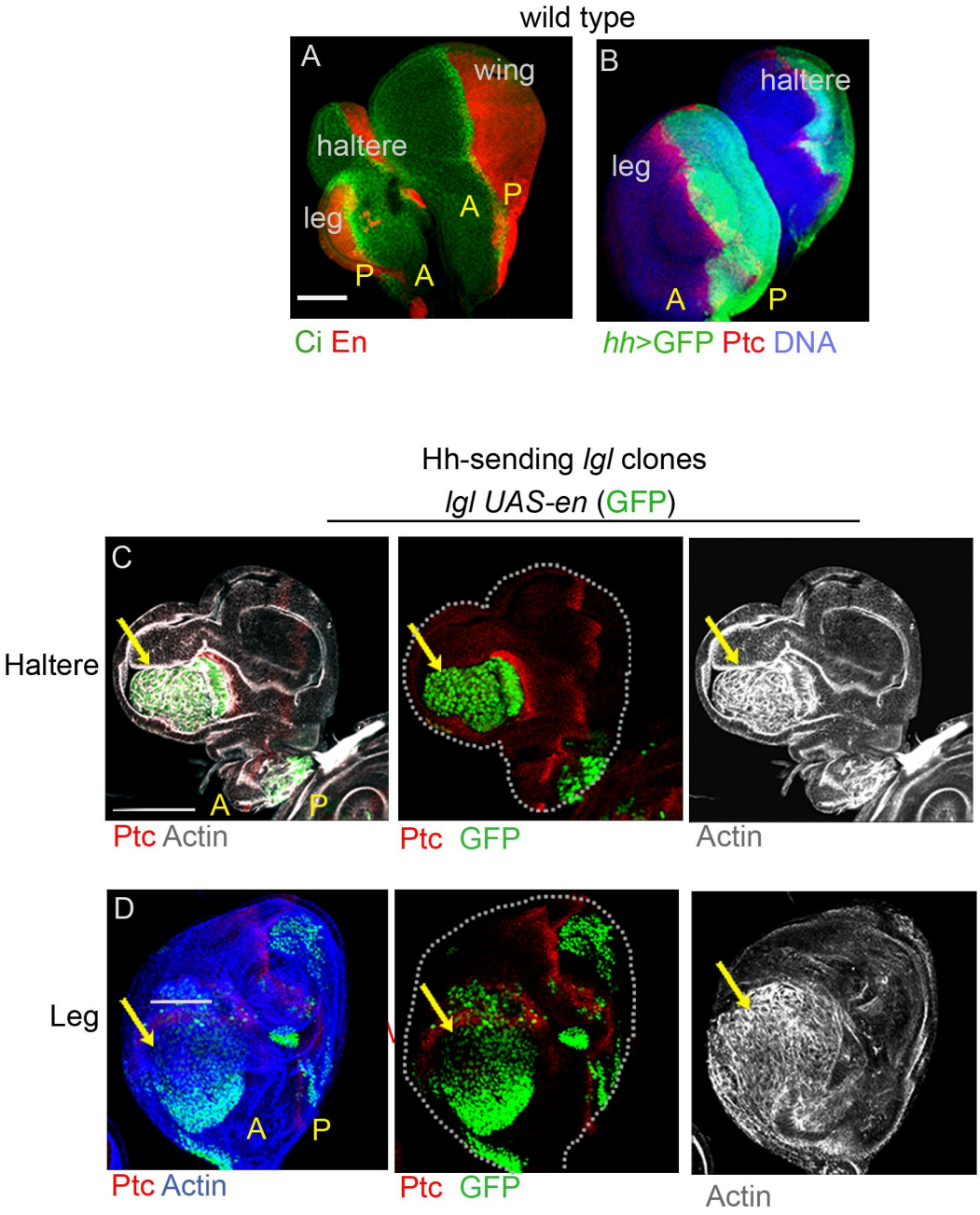
wild type
A
wing
haltere
leg
A
P
P
A
Ci En
B
haltere
leg
A
P
hh>GFP Ptc DNA
Hh-sending lgl clones
lgl UAS-en (GFP)
Haltere
C
A
P
Ptc Actin
Ptc GFP
Actin
Leg
D
A
P
Ptc Actin
Ptc GFP
Actin

FIGURE S4

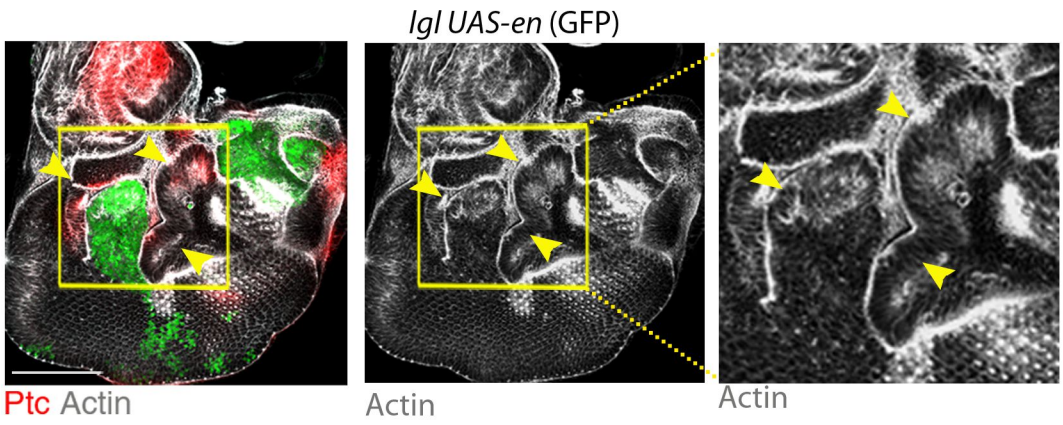

FIGURE S5

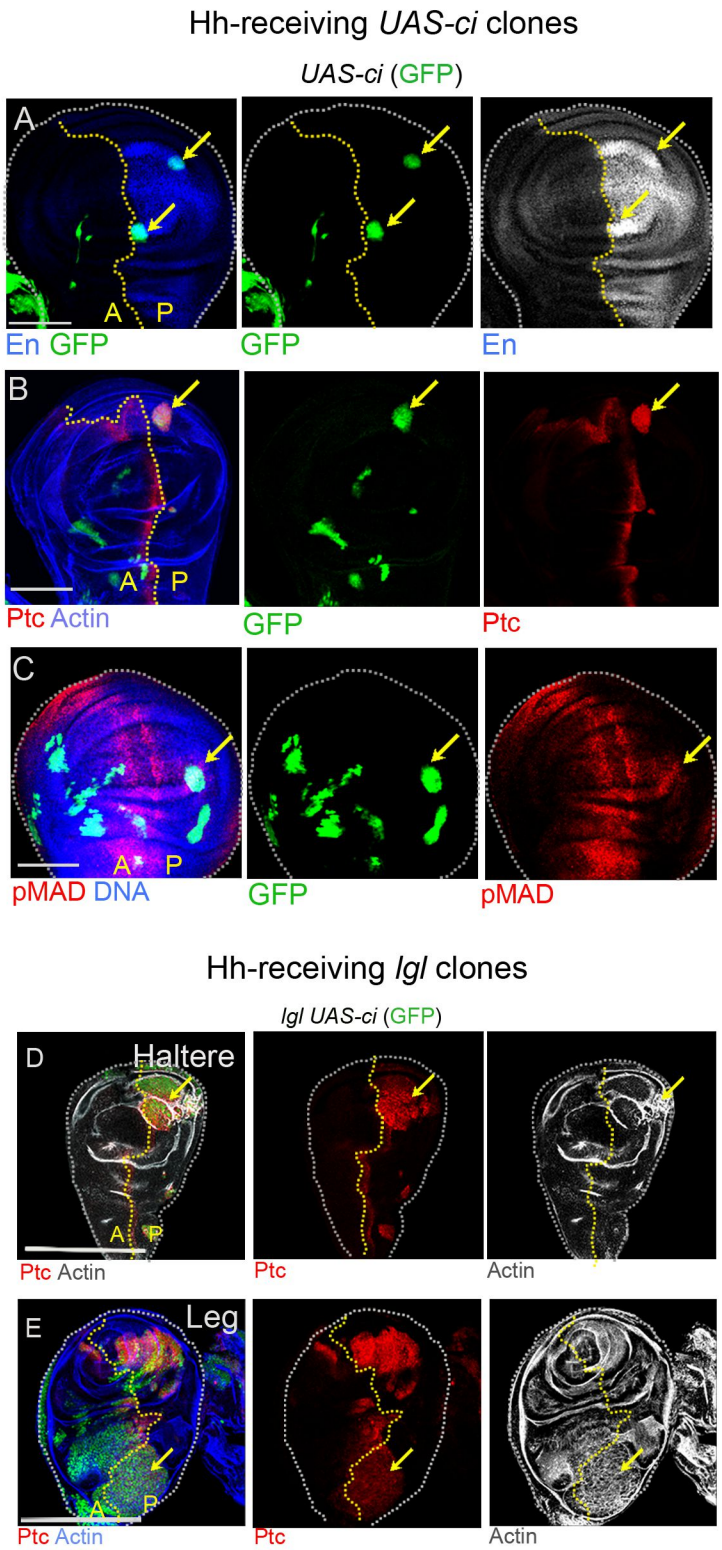
Hh-receiving *UAS-ci* clones
*UAS-ci* (GFP)
A
A P
En GFP
GFP
En
B
A P
Ptc Actin
GFP
Ptc
C
A P
pMAD DNA
GFP
pMAD
Hh-receiving *lgl* clones
*lgl UAS-ci* (GFP)
D
Haltere
A P
Ptc Actin
Ptc
Actin
E
Leg
A P
Ptc Actin
Ptc
Actin

**Table1: RESOURCE TABLE**

| REAGENTS/ RESOURCE | SOURCE | IDENTIFIER | |
|---|---|---|---|
| Experimental Models: Organisms/Strains: *Drosophila melanogaster* | | | |
| *lgl*$^{4}$ | (Khan et al., 2013) | - | |
| *UAS-yki* | (Huang et al., 2005) | - | |
| *UAS-ci* | (Methot and Basler, 1999) | - | |
| *UAS-en* | (Tabata et al., 1995) | - | |
| *UAS-ptc* | Bloomington Drosophila stock center | BDSC_5817 | |
| *tkv*$^{4}$ | Bloomington Drosophila stock center | BDSC_58786 | |
| **Antibodies** | | | **working dilution** |
| Anti-Engrailed/Invected | DSHB* | 4D9 | 1:50 |
| Anti-Ci | DSHB | 2A1 | 1:50 |
| Anti-Ptc (extracellular region) | DSHB | Apa 1 | 1:50 |
| Anti-Wg | DSHB | 4D4 | 1:250 |
| Anti-Elav | DSHB | 9F8A9 | 1:200 |
| Anti-pSmad | Cell Signaling Technology | #8828 | 1:200 |
| Anti–β-gal | Sigma-Aldrich | SAB4200805 | 1:500 |
| Anti-Lgl | Gift from Fumio Matsuzaki | - | 1:300 |
| Anti-Vg | Gift from Sean Carroll | - | 1:100 |

| | | | | |
|---|---|---|---|---|
| Alexa Fluor Phalloidin-633 | Invitrogen | A22284 | 1:100 |
| TO-PRO-3 | Invitrogen | S33025 | 1:300 |

DSHB*: Developmental Studies Hybridoma Bank, University of Iowa

---

| | | |
|---|---|---|
| EdU labeling Kit | Invitrogen | Click-iT |

---

## CONTACT FOR REAGENT AND RESOURCE SHARING

Further information and requests for resources and reagents should be directed and will be fulfilled by the Lead Contact, Pradip Sinha (pradips@iitk.ac.in)

**Genotypes of clones used in this study**

**FIGURE 1**

***lgl*⁻ clones with gain of Yki**

***1.*** *w hs-flp tub-Gal4UAS-GFP*; *lgl$^{4}$ FRT40;UAS-yki/tub-Gal80 FRT40* (Fig. 1F,G)

**FIGURE 2 and FIGURE 3**

**Hh ligand-sending *lgl*⁻ clones:**

1. *y w hs-flp tub-Gal4 UAS-GFP; lgl$^{4}$ FRT40;UAS-en/tub-Gal80 FRT40* (Fig. 2A-J, Fig. 3C-E).

***Hh ligand-sending lgl clones arrested for Hh signaling***

2. *y w hs-flp tub-Gal4 UAS-GFP; lgl$^{4}$ FRT40;UAS-en UAS-ptc/tub-Gal80 FRT40* (Fig. 2K, L).

***Hh ligand-sending lgl clones arrested for Dpp signaling***

3. *y w hs-flp tub-Gal4 UAS-GFP; lgl$^{4}$ tkv$^{4}$FRT40;UAS-en/tub-Gal80 FRT40* (Fig. 2M).

**FIGURE 3 and FIGURE 4**

**Hh ligand-receiving *lgl* clones:**

4. *y w hs-flp tub-Gal4 UAS-GFP; lgl$^{4}$ FRT40;UAS-ci/tub-Gal80 FRT40* (Fig. 3F,G; Fig. 4A-D)

***Hh ligand-receiving lgl clones arrested for Hh signaling***

5. *y w hs-flp tub-Gal4 UAS-GFP; lgl$^{4}$ FRT40;UAS-ci UAS-ptc/tub-Gal80 FRT40* (Fig.4F).

***Hh ligand-receiving lgl clones arrested for Dpp signaling***

6. *y w hs-flp tub-Gal4 UAS-GFP; $lgl^4 tkv^4$FRT40;UAS-ci/tub-Gal80 FRT40* (Fig. 4G).

**FIGURE S1**

**Loss-of-function clone of *lgl*** in a genetic background that alleviates tissue surveillance/cell competition.

*y w hs-flp; $lgl^4$ FRT40/M, arm-lacZ FRT40.* (Fig. S1B,C).

**FIGURE S2**

**Control clones**

1. *y w hs-flp; UAS-ci/act>y+>Gal4 UAS-GFP*

**FIGURE S3:**

1. *lgl* clones with constitute gain of Dpp signaling:
   *y w hs-flp tub-Gal4 UAS-GFP; $lgl^4$ $tkv^{QD}$ FRT40;* (Fig. 3A)
2. *lgl* clones blocked for Dpp reception: *y w hs-flp tub-Gal4 UAS-GFP; $lgl^4$ $tkv^4$FRT40.* (Fig. 3B)

**FIGURE S4:**

**Control clones**

**3.** *y w hs-flp; UAS-en/act>y+>Gal4 UAS-GFP*


**Dominguez, M., Brunner, M., Hafen, E. and Basler, K.** (1996). Sending and receiving the hedgehog signal: control by the Drosophila Gli protein Cubitus interruptus. *Science* **272**, 1621-5.

**Huang, J., Wu, S., Barrera, J., Matthews, K. and Pan, D.** (2005). The Hippo signaling pathway coordinately regulates cell proliferation and apoptosis by inactivating Yorkie, the Drosophila Homolog of YAP. *Cell* **122**, 421-34.

**Khan, S. J., Bajpai, A., Alam, M. A., Gupta, R. P., Harsh, S., Pandey, R. K., Goel-Bhattacharya, S., Nigam, A., Mishra, A. and Sinha, P.** (2013). Epithelial neoplasia in Drosophila entails switch to primitive cell states. *Proc Natl Acad Sci U S A* **110**, E2163-72.

**Methot, N. and Basler, K.** (1999). Hedgehog controls limb development by regulating the activities of distinct transcriptional activator and repressor forms of Cubitus interruptus. *Cell* **96**, 819-31.

**Subramanian, A., Tamayo, P., Mootha, V. K., Mukherjee, S., Ebert, B. L., Gillette, M. A., Paulovich, A., Pomeroy, S. L., Golub, T. R., Lander, E. S. et al.** (2005). Gene set enrichment analysis: a knowledge-based approach for interpreting genome-wide expression profiles. *Proc Natl Acad Sci U S A* **102**, 15545-50.

**Tabata, T., Schwartz, C., Gustavson, E., Ali, Z. and Kornberg, T. B.** (1995). Creating a Drosophila wing de novo, the role of engrailed, and the compartment border hypothesis. *Development* **121**, 3359-69.

**Tanimoto, H., Itoh, S., ten Dijke, P. and Tabata, T.** (2000). Hedgehog creates a gradient of DPP activity in Drosophila wing imaginal discs. *Mol Cell* **5**, 59-71.

**van den Heuvel, M., Harryman-Samos, C., Klingensmith, J., Perrimon, N. and Nusse, R.** (1993). Mutations in the segment polarity genes wingless and porcupine impair secretion of the wingless protein. *EMBO J* **12**, 5293-302.

**Zecca, M., Basler, K. and Struhl, G.** (1995). Sequential organizing activities of engrailed, hedgehog and decapentaplegic in the Drosophila wing. *Development* **121**, 2265-78.